



ELSEVIER

Physica A 270 (1999) 295–300

PHYSICA A

www.elsevier.com/locate/physa

Melting driven by particle size-dispersity: a study in two dimensions

M.R. Sadr-Lahijany^a, P. Ray^{b,*}, H.E. Stanley^a

^a*Center for Polymer Studies and Department of Physics, Boston University, Boston, MA 02215, USA*

^b*The Institute of Mathematical Sciences, Chennai 600 113, India*

Abstract

We study the effect of particle size-dispersity on solids and melting of solids by molecular dynamics simulation on a two-dimensional size-dispersed Lennard-Jones system. We find that size-dispersity disfavors solidification and on increasing the dispersity, the solid ‘melts’, at a critical dispersity, to a liquid. The solid–liquid transition depends on the density — the transition is continuous through the ‘hexatic’ phase at low densities and abrupt first order transition at higher densities. We find that size-dispersity creates topological defects in the close-pack solid structure which destroy the crystalline order in solids. © 1999 Elsevier Science B.V. All rights reserved.

PACS: 64.70.Dv; 61.20.Ja; 64.60.Cn

Keywords: Size-dispersity; Melting transition; Hexatic phase; Topological defects

Ordering and melting of crystals have long attracted attention of the scientific community. It is still not clear what exactly causes melting and the question is even more important for melting in two dimensions, where the nature of the transition (a continuous transition through the ‘hexatic’ phase or a discontinuous transition) is always debated [1]. A milestone of our understanding of crystal ordering is perhaps the Kirkwood–Alder transition which shows that packing of non-interacting hard (impenetrable) spheres alone can cause ordering with the absence of any latent heat upon crystallization. The situation is very much realizable in colloidal suspensions and the computer-simulated equation of state for hard spheres [2,3] was verified by X-ray densitometry of polystyrene spheres in salt solution [4].

* Corresponding author.

E-mail address: ray@imsc.ernet.in (P. Ray)

A well-known example of ordered colloidal crystal is opal – formed from the compression of two kinds of silica spheres of different sizes over geological timescales. There are many such examples of colloids where particles have different sizes. Studies reveal that the structure and stability of a crystal depend critically on the difference in particle sizes [5–9]. Size-dispersity disfavours solidification and as dispersity is raised, the liquid is to be compressed (or equivalently, the temperature is to be lowered) more and more to achieve crystallization. Above a critical dispersity, the solid becomes unstable and crystallization becomes impossible. Computer simulation studies show that the above feature of size-dispersity is valid in two and three dimensions, for various form of size-distribution and inter-particle interactions [10].

All these studies leave few questions unanswered: (i) what are the different phases that may appear when size-dispersity is present in the system (ii) what happens when starting from the solid phase, size-dispersity is slowly introduced leaving other thermodynamic parameters unchanged (iii) what happens when dispersity crosses the threshold value beyond which solid is unstable and (iv) how solid order is affected in close-packing of particles when some of the particles have different sizes. These are the questions we address here by studying a Lennard-Jones system in two dimensions by molecular dynamics simulation.

We simulate $N = 10^4$ particles interacting with a truncated ‘shifted-force Lennard-Jones’ pair-potential [11]. We introduce size dispersity by choosing half of the particles smaller than the rest, and define Δ to be the ratio of the difference in their sizes to the mean size. We start by placing the particles randomly on the sites of a triangular lattice embedded in a rectangular box of edges L_x , L_y and aspect ratio $L_x/L_y = \sqrt{3}/2$. We use the velocity Verlet method to integrate Newton’s equation of motion. Units are set by choosing the mass of the particles and the Lennard-Jones energy scale to be unity. The simulation is run typically for 2×10^5 MD time steps, where we have chosen the time step to be 0.01. We define the density ρ to be the ratio of the area occupied by the particles to the box area. A state, defined by ρ and Δ , is first equilibrated at a constant temperature $T = 1$ using Berendsen’s thermostat [11]; at this temperature the 2D-solid can be formed at low enough dispersity. The simulation is then run at constant energy until the temperature T , pressure P and the energy E stabilize with less than 1% fluctuation. We start with a low density in the liquid state. Higher density states are obtained by gradually compressing the box, keeping the aspect ratio fixed. We increase ρ from 0.85 to 1.05 through 20 intermediate densities, equilibrating the system at each of these densities.

In Fig. 1 the average virial pressure P is shown for state point versus ρ for constant Δ . The graph for $\Delta = 0$ has the low density liquid branch and the high density solid branch joined by a plateau. Upon increasing Δ , the liquid branch extends to larger values of ρ and the solid branch is shifted to larger values of P for the same value of ρ . The significant observation is that the plateau between the two branches narrows down upon increasing Δ and at around $\Delta_{th} \approx 0.1$ the plateau disappears completely. What the equation of state graphs of Fig. 1 imply is that for $\Delta > \Delta_{th}$, there is no density driven liquid–solid transition.

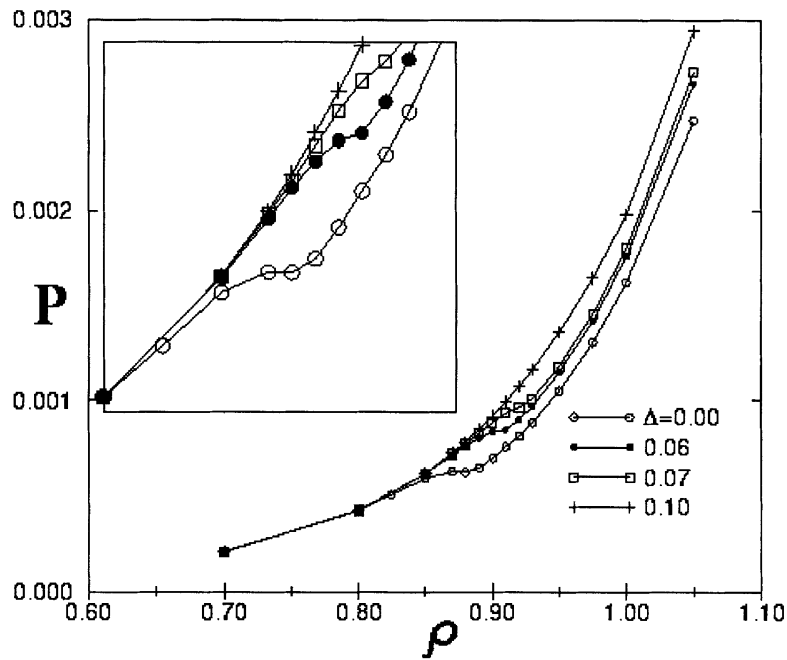


Fig. 1. The equation of state for different values of Δ . The lowest curve, corresponding to the monodispersity ($\Delta = 0$) exhibits a distinct plateau between the low density (liquid) and high density (solid) regions. The plateau gradually weakens upon increasing Δ and vanishes for $\Delta \geq 0.10$ (magnified at the inset).

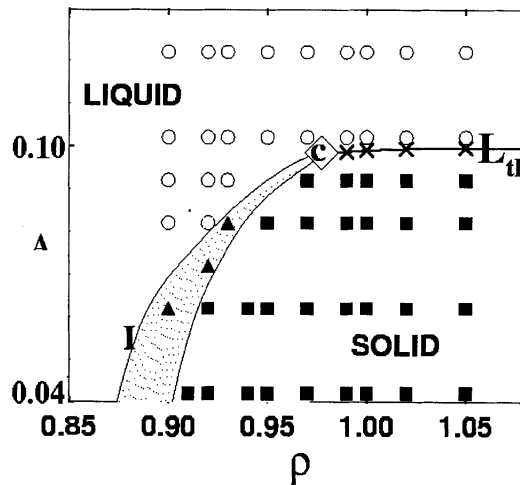


Fig. 2. Phase diagram in the $\Delta - \rho$ parameter space. Squares represent solid points and circles liquid points. The threshold line L_{th} connects crosses, which are the first order phase transition points. The triangles are the points of the intermediate (I) phase, showing a hexatic behavior. The large diamond marks the possible multicritical point C at the junction of first and second order transitions.

Liquid has all the symmetries of the free space, while in solid the symmetries are reduced. Solid has long-range (or quasi long range in two dimensions) translational and orientational order. The pair correlation function, $g(r)$, serves to specify the degree of translational order by measuring the distance dependence of static two-point correlations in the density. The solid is distinguished by having a periodic $g(r)$ with non vanishing

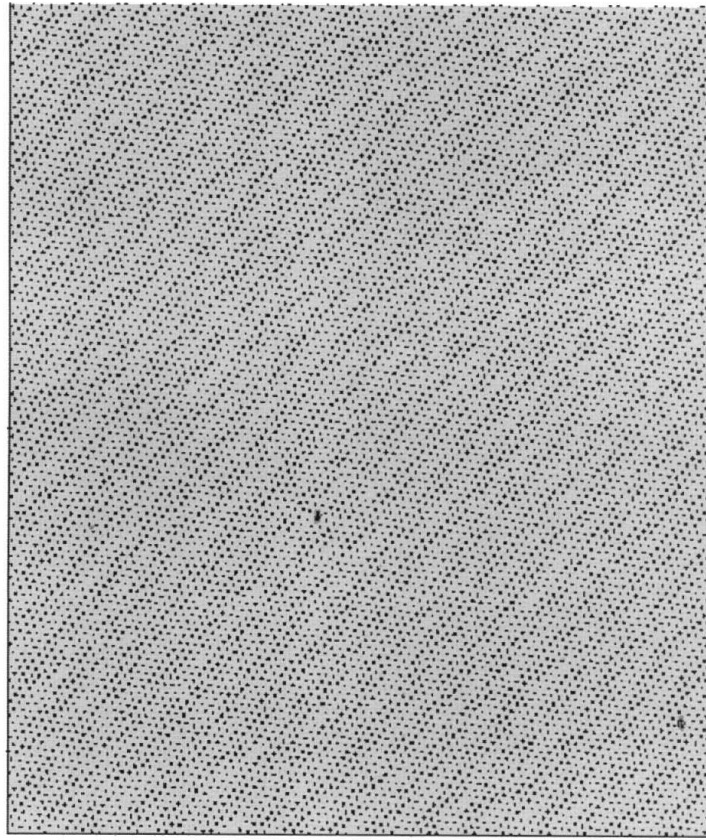


Fig. 3. The defect structure at $\rho = 1.0$ and $\Delta = 0.4$ which is deep in the solid phase. Only few quadrupoles are present. The arrows are the dipoles or dislocations and two side by side arrows pointed in the opposite directions constitute a quadrupole.

amplitude which extends to $r \rightarrow \infty$. For liquid, on the other hand, $g(r) \rightarrow 1$ as $r \rightarrow \infty$, which reflects the uniformity of the density distribution. For small r , $g(r)$ shows the exponential decay with a characteristic length ξ representing a short range order around each particle. Besides translational order, liquids and solid are different in their transformation properties under rotation. While liquids are characterized by uniform distribution of mass and as a result they are invariant under continuous rotations, this symmetry is broken for the lattice like solid. For example a $2D$ closed packed solid which is in the form of a triangular lattice is invariant only under rotations that are multiples of 60° . While in a crystal the translational and rotational order occur simultaneously, this need not always to be the case. In $2D$, there may exist a ‘hexatic’ phase [1,12,13] which lacks any translational order, but shows some type of orientational order. One can measure the local orientational order ψ_6 by quantifying the degree of ‘hexagonality’ of the nearest neighbor around each particle, $(\psi_6)_j \equiv \frac{1}{z} \sum_{k=0}^z e^{i6\theta_{jk}}$, where the sum runs over all z nearest neighbors k of j , and θ_{jk} is the angle of the bond joining particles j and k with respect to a fixed axis. We identify nearest neighbors by constructing the Voronoi lattice. The modulus of $(\psi_6)_j$ will be unity if the neighbors form a perfect hexagon around j . For a distorted hexagon or a different polygon, $|(\psi_6)_j| < 1$ [14]. The orientational correlation $g_6(r) = \langle \psi_6(0)\psi_6(r) \rangle$ shows long range order in the solid

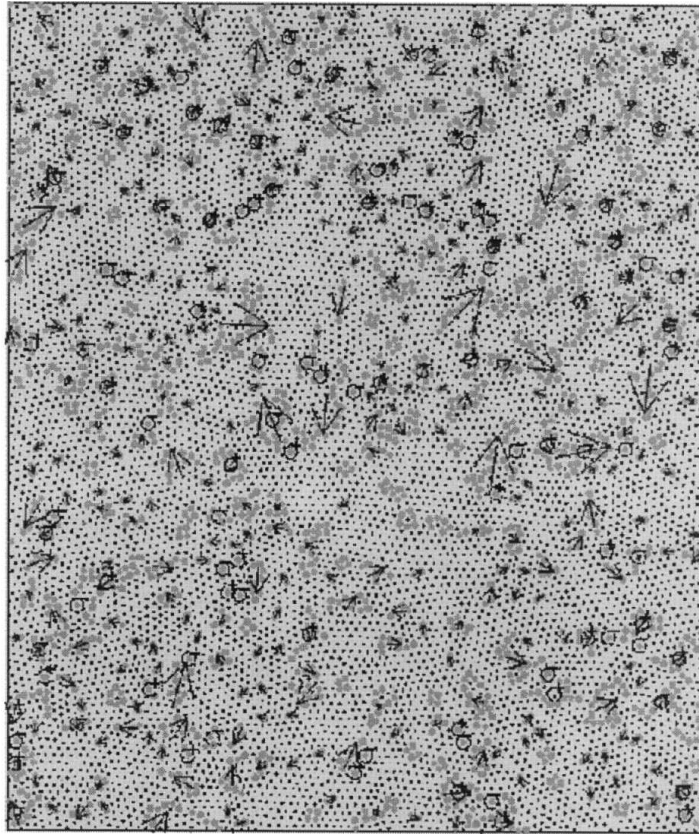


Fig. 4. The defect structure at $\rho = 1.0$ and $\Delta = 1.07$ which is in the liquid phase. All kinds of defects are present. The arrows represent the dislocations and the circles represent the disclinations. A big cluster may have a net dipole moment of larger magnitude given by a long arrow.

phase, falls exponentially in the liquid phase and decays algebraically in the hexatic phase. These two correlations tell us the nature of the different phases that appear as size-dispersity is introduced.

From the determination of various phases we arrive at the phase diagram presented in Fig. 2. What the diagram reveals is that for high densities $\rho > \rho_{th} \approx 0.95$, the solid and liquid phases are separated by a line L_{th} of first order transition as one changes the dispersity. On the other hand, for lower densities in the range $0.9 < \rho < \rho_{th} \approx 0.95$, the solid and liquids are separated by an intermediate hexatic phase and the dispersity driven melting is a continuous three phase (solid-hexatic-liquid) transition.

We look for the defects that destroy crystalline order. The defects can be detected by looking into the nearest neighbors of a particle which is obtained by Voronoi construction. In two dimensions, the close-packed structure is hexagonal. A defect arises when a particle has $n \neq 6$ neighbors, which generates a ‘topological charge’ $q = n - 6$ [14]. Two or more such defects can reside side by side in a cluster with total charge $Q \equiv \sum q_i$ and dipole-moment $\mathbf{P} \equiv \sum \mathbf{r}_i q_i$ (for each cluster, the sum is over all its defects i at position \mathbf{r}_i with charge q_i). We find that the defects fall in *three* categories. (i) *Disclinations*. Free charges, with $q = \pm 1$ corresponding to whether a particle is five- or seven-fold coordinated; larger particles generally acquire a positive charge and

the smaller ones acquire a negative charge. (ii) *Dislocations*. Dipoles composed of a bound pair of disclinations of opposite charge, formed by neighboring large and small particles with seven and five neighbors, respectively. (iii) *Blobs*. Defect clusters with zero charge and dipole moment, most common being quadrupoles made of a bound pair of dislocations with opposite dipole moments (see eg. [15]). The quadrupole has neither charge nor dipole moment and they do not destroy the translational or orientational order, so they are energetically not expensive. In Fig. 3, we find these are the defects which are mostly present deep in solid phase. Whereas in liquid phase, from Fig. 4, we find that defects of all the three kinds are present. Dislocations destroy the translational order and disclinations destroy the orientational order. So in their presence liquid phase loses both these orders.

References

- [1] K.J. Strandburg, Rev. Mod. Phys. 60 (1988) 207.
- [2] B.J. Alder, T.E. Wainwright, Phys. Rev. 127 (1962) 359.
- [3] B.J. Alder, W.G. Hoover, D.A. Young, J. Chem. Phys. 49 (1968) 3688.
- [4] A.P. Gast, W.B. Russel, Phys. Today (December 1998) 24.
- [5] E. Dickinson, R. Parker, M. Lal, Chem. Phys. Lett. 79 (1981) 578.
- [6] E. Dickinson, R. Parker, J. Physique Lett. 46 (1985) L229.
- [7] J.L. Colot, M. Baus, Mol. Phys. 56 (1985) 807.
- [8] J.L. Barrat, J.P. Hansen, J. Physique 47 (1986) 1547.
- [9] P.N. Pusey, J. Physique 48 (1987) 709.
- [10] W. Vermohlen, N. Ito, Phys. Rev. E 51 (1995) 4325.
- [11] M.P. Allen, D.J. Tildesley, Computer Simulation of Liquids, Oxford University Press, New York, 1989.
- [12] B.I. Halperin, D.R. Nelson, Phys. Rev. Lett. 41 (1978) 121.
- [13] D.R. Nelson, in: C. Domb, J.L. Lebowitz (Eds.), Phase Transitions and Critical Phenomena, vol. 7, Academic Press, London, 1983, p. 1.
- [14] M.A. Glaser, N.A. Clark, in: I. Prigogine, S.A. Rice (Eds.), Advances in Chemical Physics, vol. 83, Wiley, New York, 1993, p. 543.
- [15] D.R. Nelson, M. Rubinstein, F. Spaepen, Philos. Mag. A 46 (1982) 126.